



A comparison of quality control methods for active coating processes

D. Brock^a, J.A. Zeitler^b, A. Funke^c, K. Knop^a, P. Kleinebudde^{a,*}

^a Institute of Pharmaceutics and Biopharmaceutics, University of Düsseldorf, Universitätsstrasse 1, 40225 Düsseldorf, Germany

^b Department of Chemical Engineering and Biotechnology, University of Cambridge, Pembroke Street, Cambridge CB2 3RA, United Kingdom

^c Global Chemical & Pharmaceutical Development, Bayer Pharma AG, Müllerstrasse 178, 13353 Berlin, Germany

ARTICLE INFO

Article history:

Received 19 July 2012

Received in revised form 5 September 2012

Accepted 8 September 2012

Available online 16 September 2012

Keywords:

Terahertz pulsed imaging

Active coating

Coating thickness

Pan coating

Optical microscopy

ABSTRACT

Terahertz pulsed imaging (TPI) is a recent and nondestructive technique to quantify coating thickness of pharmaceutical tablet film coatings. In this study, TPI is used for the first time to quantify the progress of an active coating process. The dosage form consisted of a push–pull osmotic system comprising a two-layer tablet core with a functional film coating and a laser drilled hole. On top of this system an active coating was applied. The coating thickness data acquired by TPI and optical microscopy was compared to the quantification of the active pharmaceutical ingredient (API) via HPLC. Good correlation of TPI and HPLC data was shown for coating thicknesses up to 500 μm . Due to the special structure of the dosage form, the TPI detection limit of 38 μm layer thickness was circumvented by analysing the coating thickness of active coating and functional subcoat in one. Therefore it was possible to monitor the active coating process from the very beginning of the process. Optical microscopy was no suitable reference technique for TPI thickness measurements. The active coating showed deformation artefacts during sample preparation, which biased the subsequent thickness measurements.

© 2012 Elsevier B.V. All rights reserved.

1. Introduction

Polymer film coating of tablets is a common technique in the processing of solid oral dosage forms. Coatings are applied for a number of reasons, for example taste-masking, light-protection or the modified release of the active pharmaceutical ingredient (API) from the tablet core. Furthermore, APIs can be mixed with the coating polymer and incorporated into the coating layer. Such formulations can be used to obtain a combination of different release profiles (e.g. immediate release from the coating followed by extended release from a tablet matrix) or to combine different drugs in one dosage form while avoiding potential incompatibility. Active coating is also suitable for low-dose formulations (Barcomb, 1997; Fricke, 2006).

Dosage forms with an active film coating need to meet the requirements on uniformity of dosage units according to the pharmacopoeia (USP<905>, Ph.Eur.2.9.40). In order to achieve this aim, it is important to meet the target API content accurately and to produce batches with high coating uniformity. Therefore, the quantification of the coating process and the definition of the coating endpoint are crucial.

Process control via weight gain of the tablets is prone to error due to the variability in weight of the tablet cores. In addition the results can be further biased by residual solvent content in the coating layer directly after the coating process. Therefore, it would be desirable to use continuous and robust measurement techniques that make it possible to follow the coating process non-destructively and in real time. Methods based on NIR and Raman spectroscopy have attracted considerable attention in this context as they can be applied as in-line process analytical technology (PAT) tools to determine the coating endpoint (De Beer et al., 2011; Gendre et al., 2011; Müller et al., 2010a,b).

Terahertz pulsed imaging (TPI) is a recent non-destructive measurement technique that can be used to determine the coating thickness on pharmaceutical tablets. As an imaging technique it can spatially resolve the distribution of the coating layer over the entire surface of a tablet. The technique works by using short pulses of terahertz radiation (full width at half maximum (FWHM) <1 ps), that are focused onto the surface of a tablet. Polymers are semitransparent to terahertz radiation and hence a part of the pulse can penetrate into the coating while the other part of the pulse is reflected to the detector. At every subsequent interface where a change in refractive index occurs, further parts of the pulse are reflected back and can be detected as additional reflection pulses (Fig. 1). Using the time delay between the reflection pulses, the coating thickness d_{coat} of the material can be calculated as $2d_{\text{coat}} = \Delta t c/n$, where Δt is the time delay between two reflection pulses, c is the speed of light and n the refractive index of the coating

* Corresponding author. Tel.: +49 211 14220; fax: +49 211 14251.

E-mail addresses: daniela.brock@uni-duesseldorf.de (D. Brock), jaz22@cam.ac.uk (J.A. Zeitler), adrian.funke@bayer.com (A. Funke), klaus.knop@uni-duesseldorf.de (K. Knop), kleinebudde@uni-duesseldorf.de (P. Kleinebudde).

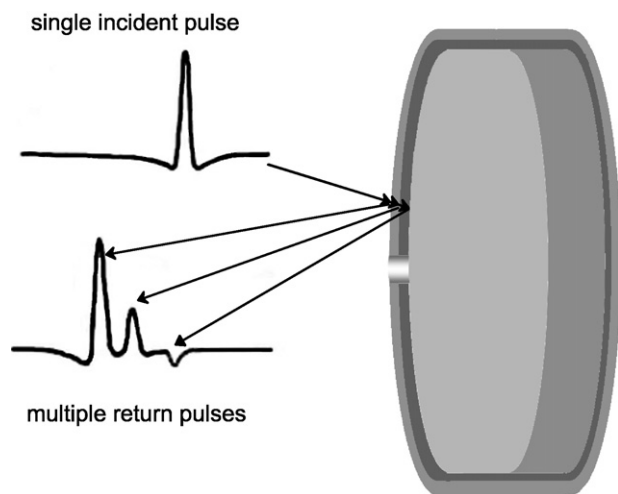


Fig. 1. Schematic of the TPI measurement on an individual sampling point. Depicted is the single incident terahertz pulse and the multiple return pulses created by the interface reflections of the radiation. The schematic does not display the precise tablet and film thickness dimensions. For further details see Section 2.

material. Detailed information about the measurement technique is provided by Zeitler et al. (2007b).

The coating thickness measurements obtained by TPI were compared to microscopic reference data and good agreement was found (Ho et al., 2007). Using this technique it was possible to monitor the growth of the coating layer with process time during a coating run in off-line measurements. The coating interface peaks were found to separate from the tablet surface peaks with coating time, indicating the growth of the coating layer (Ho et al., 2009). The technology has since been developed further, and, using a prototype in-line gauge, it was demonstrated that this technology can be used to measure the coating thickness of individual tablets during a coating run (May et al., 2011). The acquired thickness data showed good agreement with tablet weight gain but the real potential of the TPI measurement lies in its ability to resolve the tablet-to-tablet coating thickness distribution within the coating drum at any time during the process.

However, TPI is still a very recent measurement technique and further testing of the technique is required before it can be applied more widely. At present the measurement of the coating thickness is only possible when surface and interface reflection peaks are clearly resolved, which translates into a detection limit of approximately 38 μm coating thickness. There are no reports on the applicability of TPI measurements for thick coating layers (>200 μm) or active coating processes, yet.

The aim of this study was the quantification of the progress of an active coating process up to a coating thickness of approximately 500 μm and to evaluate how the coating thickness measurements correlate with API content in an active coating. The TPI data should further be compared to optical microscopy as a destructive reference technique.

2. Materials and methods

2.1. Film coating

For the active coating, push–pull osmotic systems, comprising a two-layer tablet core with a functional polymer coating and a laser drilled hole, were used as starting materials (Bayer Pharma AG, Berlin, Germany). The two layers of the tablet core are characterised by different colours, i.e. yellow for the tablet layer with the laser drilled hole and red for the other layer. The tablet diameter of the cores before coating was 8.4 mm. The coating suspension consisted

Table 1
Process parameters in the active coating process.

Parameters		
Tablet cores	3	kg
Spray rate (0–60 min)	8	g/min
Spray rate (60–348 min)	12	g/min
Drum rotation speed	18	rpm
Inlet air volume	140	m^3/h
Outlet air temperature	45	$^{\circ}\text{C}$
Atomization air	0.8	bar
Forming air	1.0	bar

of 4 parts (m/m) micronized candesartan cilexetil as API (Bayer Pharma AG, Berlin, Germany), 6 parts (m/m) polyvinyl alcohol (PVA) based polymer mixture (Colorcon, Dartford, UK) and 24 parts (m/m) of water, leading to a suspension with 29.41% solids content. Candesartan cilexetil was first suspended in water using an Ultra-Turrax homogenizer (Janke und Kunkel KG, Staufen, Germany). Subsequently, the PVA based polymer mixture was added and the mixture was stirred with a paddle stirrer in an ultrasound bath for 90 min until all polymer particles had dissolved. The suspension was filtered through a 315 μm sieve prior to the coating process. Film coating was performed in a side-vented pan coater (BFC5, L.B. Bohle, Ennigerloh, Germany) at 3 kg scale. Process parameters are listed in Table 1. Approximately 30 tablets were taken every 30 min throughout the whole coating process with additional sampling points at 10, 50 and 339 min coating time and at coating endpoint (348 min).

2.2. Terahertz pulsed imaging

Tablets were analysed by TPI using a TPI imaga 2000 system (TeraView Ltd., Cambridge, UK). Of both, the starter cores (0 min process time) and the final product (348 min process time), 36 tablets were measured in full scan mode. A measurement consisted of scanning both faces of the tablet as well as the centre band with a spot size of 200 \times 200 μm and a penetration depth of 2 mm in air. The data acquisition time was 50 min per tablet. In addition, six tablets were measured at each sampling point in the range of 10–339 min process time. For these measurements the radius of the circular sampling area on the surface of each tablet was limited to 3 mm of each tablet face to reduce data acquisition time to 20 min per tablet. No data was acquired from the centre band in these samples. Coating thickness analysis was performed using TPIView software version 3.0.3 (TeraView Ltd., Cambridge, UK). As the real refractive index n_{real} of the film coating was unknown, it was set to $n_{\text{estimated}} = 1.53$, which is the refractive index of polyethylene. Matlab version R2009a (Mathworks, Ismaning, Germany) was used for any subsequent numerical analysis. For the data analysis all pixels on the tablet edges as well as the pixels in the region of the laser drilled hole were excluded to avoid scattering artefacts. The region of interest (ROI) was defined by a torus of 1.5 mm inner radius and 3 mm outer radius with reference to the centre of the tablet face, including approximately 500 data points per tablet face. The torus shape guaranteed that no pixels with signal distortions in the hole region were included in the analysis. For consistency, the same ROI was applied to both tablet faces. The differences in resulting coating thickness on the red face of the tablet, which did not contain a hole, were insignificant regardless as to whether a torus shaped ROI or a circular one was applied.

2.3. Optical microscopy

Following TPI analysis, three of the six tablets per sampling point (10–339 min process time) were cut into halves using a tablet divider (Exakt Tablettenteiler, MEDA GmbH & Co. KG, Bad

Homburg, Germany). Cutting the tablets using the tablet divider resulted in smooth cut surfaces on the face of the tablet on which the blade was positioned indicating a plastic deformation. On the other tablet face coarse cut surfaces were obtained indicating a brittle fracture. In order to avoid this artefact, the tablets were tried to freeze in liquid nitrogen prior to cutting. However, while avoiding plastic deformation, this method led to extensive delamination of the coating which was equally unsuitable for subsequent quantitative analysis. Microscopy measurements were performed at 10-fold magnification (Leica DMLB, Leica Microsystems, Wetzlar, Germany) and the coating thickness was measured using the Leica software QWin Lite V2.3 (Leica Microsystems Imaging Solutions, Wetzlar, Germany). 30 Data points were measured per tablet face and the mean thickness and standard deviation was calculated using Origin Pro 8G software (OriginLab Corporation, Northampton, USA).

2.4. Cryomicrotome sample preparation

Cryomicrotome preparation was performed on a single tablet to evaluate the general applicability of this method. Here, a 5% carboxymethyl cellulose (CMC) solution was used as embedding medium for the tablet. A CMC block with indentations for the tablet samples was frozen at -70°C and tablets were embedded followed by adding fresh CMC solution to the indentations in order to fill the gaps. The sample block was then warmed up to -25°C and slices of $10\ \mu\text{m}$ thickness were prepared using a cryomicrotome with included freeze-drier (Leica CM3600, Leica Microsystems, Wetzlar, Germany). The 12 slices that were located closest to the drilling region were used for thickness analysis using optical microscopy as outlined above.

2.5. HPLC analysis

The total candesartan cilexetil (CAN) content in the coating was determined by high performance liquid chromatography (HPLC) analysis in all samples following optical microscopy analysis (Elite LaChrom, VWR Hitachi, Darmstadt, Germany). In addition to the tablet halves that were obtained from the microscopy analysis, 10 tablets from the coating endpoint were analysed. The active coating layer of the individual tablets was dissolved in 10 ml water. Throughout this procedure, the push-pull osmotic system stayed intact. The solution was then filled up to 100 ml with methanol. Subsequently, the solution was filtered and a 10% dilution was prepared for HPLC analysis. For the HPLC method a C18-column (X-Bridge, Waters GmbH, Eschborn, Germany) with precolumn was used. The eluent consisted of 80% (v/v) methanol and 20% (v/v) phosphate buffer (5 mmol, pH 3). The flow rate was set to 0.6 ml/min. The oven temperature of the column was set to 40°C . Detection was achieved by measuring the UV absorption at 260 nm. Each sample was measured in triplicate and the mean content as well as the standard deviation were calculated. Data analysis was performed using EZChrom Elite software (VWR Hitachi, Darmstadt, Germany).

3. Results

All three methods, TPI, optical microscopy and HPLC, clearly show an increase in coating thickness or CAN content with process time (Fig. 2). A good agreement is found between the results from all three techniques.

As previously reported the TPI measurements require a minimum coating thickness of around $40\ \mu\text{m}$ in order to resolve the film from the tablet matrix (Zeitler et al., 2007a). The coating thickness of the tablets that were coated for less than 50 min is below the detection limit and hence TPI only provides results from 50 min

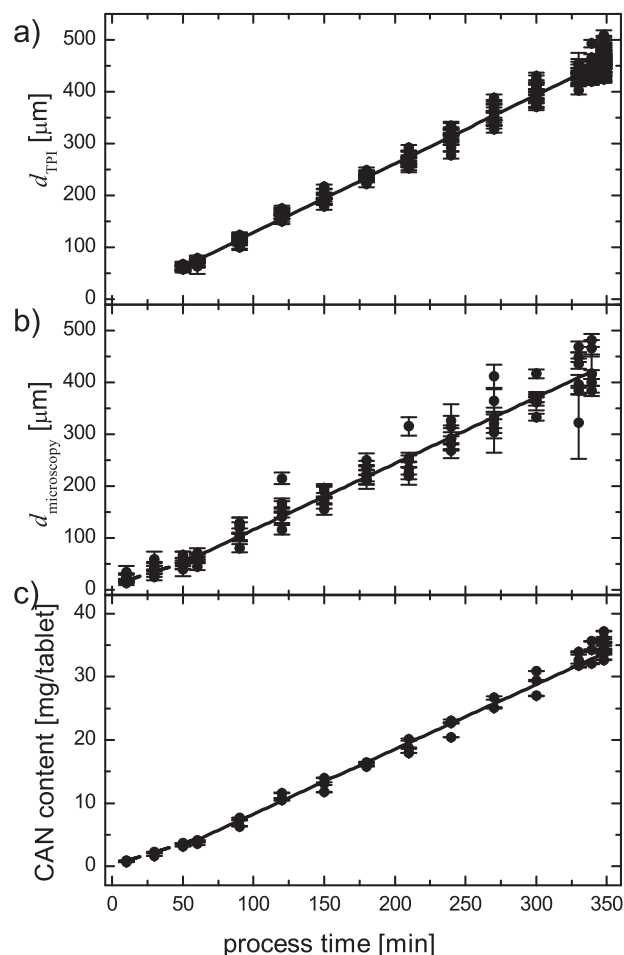


Fig. 2. Coating characteristics over process time: layer thickness of the active coating layer measured by TPI (a); microscopy (b); as well as the corresponding CAN content measured by HPLC (c).

process time onwards. In this coating process the spray rate was increased from 60 min onwards. This results in an increased slope of the corresponding regression lines after fitting a linear equation to the data points below and above 60 min process time (Table 2).

As stated in Section 2.1, two coating layers exist on top of the two-layer tablet core. Hence, two interface reflection pulses are expected in the TPI waveforms corresponding to the interfaces of the active to the functional subcoat and from the subcoat to the tablet core (cf. Fig. 1). There are distinct differences in the reflected waveforms that are acquired in the TPI measurement from the two faces of the individual tablet. On the yellow tablet face two peaks are observed that correspond to the two coating layers as anticipated (Fig. 3). Following the surface reflection peak, a positive peak is observed in the terahertz waveform, which corresponds to the interface between the active coating layer and the functional subcoat. This reflection is followed by a negative peak that corresponds to the coat/core-interface.

On the red tablet face, only the first interface peak can be resolved. The second coating interface is obscured by strong oscillations in the waveform at longer delay times. These oscillations are caused by large sodium chloride crystals in the red tablet layer, of which the diameter was in the range of the wavelength THz radiation (i.e. 60 GHz to 4 THz, 5 mm to $75\ \mu\text{m}$). The oscillations make it difficult to resolve the thickness of the functional film coating on this face of the tablet. Nonetheless, the thickness of the active coating layer can be quantified as the corresponding coating interface peak can clearly be separated from the oscillations.

Table 2
Linear regression of the coating quantity over process time using a fit to the equation $y = ax + b$ (phase 1: $0 < x \leq 60$ min process time; phase 2: $60 \leq x \leq 348$ min process time).

Technique	Phase	<i>a</i>	<i>b</i>	<i>R</i> ²	RMSE
TPI	1	–	–	–	–
	2	1.33	–4.32	0.988	15.54 μm
Microscopy	1	0.75	16.35	0.708	9.71 μm
	2	1.27	–6.98	0.943	29.15 μm
HPLC	1	0.06	0.19	0.962	0.26 mg
	2	0.11	–2.83	0.989	1.16 mg
TPI bilayer	1	1.32	196.29	0.839	12.99 μm
	2	1.33	191.64	0.975	21.29 μm

A linear increase of coating thickness over process time can be found (Fig. 2a). As the first interface peak only becomes visible at approximately 50 μm coating thickness, the process can only be followed from 50 min process time onwards. Before that timepoint, the first interface peak is overlapped by the surface reflection peak and therefore, no coating analysis can be applied to directly determine the coating thickness of the CAN layer (Fig. 4).

To circumvent this detection limit, the second interface peak was used for analysis, calculating the joint coating thickness of both coating layers. For this method, again a linear relationship of coating thickness over time was found (Fig. 5, $R^2 = 0.99$) while an increase in slope after 60 min process time cannot be found in dimensions similar to Fig. 2b and c. Layer thickness of the functional film coating prior to the active coating process was determined as 196 ± 13 μm on the yellow tablet face. As the coating thickness of the functional subcoat can be assumed to be constant during the active coating process, the layer thickness of the active coating can be calculated by subtracting the *y*-intercept of the regression line from the measured joint coating thickness. Good correlation of both single-layer and two-layer analysis was found (Fig. 6). However, this two-layer analysis can only be performed on the yellow tablet face, as the

second interface peak cannot be easily identified on the red tablet face due to the sodium chloride crystals.

The microscopy data shows high standard deviations for some tablets in comparison to the TPI data (Fig. 2a and b). Also the data spread more broadly around the regression line and a higher RMSE and lower R^2 were found for the microscopy data (cf. Table 2). When comparing the coating thickness of the tablet face where the blade was positioned (i.e. cut side), and the face where a brittle fracture occurred (i.e. break side), it is evident that the cut side exhibits higher coating thickness values in comparison to the break side (Fig. 7). This is indicative of a plastic deformation of the coating layer during the cutting process.

It was not possible to overcome this problem by freezing the tablets with liquid nitrogen to induce a brittle fracture. During the cutting process, the active coating layer delaminated, so that a homogeneous cut was not possible (Fig. 8). Using the cryomicrotome for sample preparation led to multiple brittle fractures in the coating layers, that made it difficult to acquire reliable coating thickness data. In addition, the outer coating layer started to dissolve in the CMC matrix, even though the freezing time was kept as short as possible to prevent the film coating from dissolution (Fig. 9).

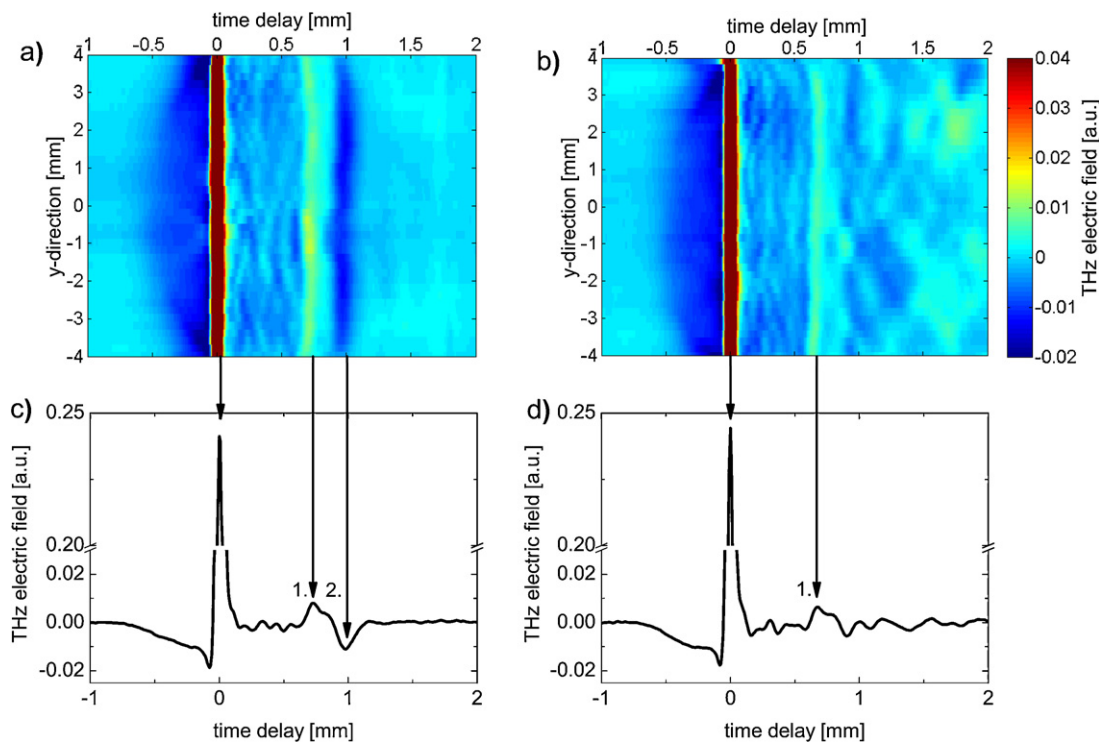


Fig. 3. Virtual cross-section (a,b) and individual time-domain waveforms acquired by TPI for yellow (c) and red (d) tablet face. Virtual cross-sections show the THz electric field in false colour map. The tablet surface (red line), first coating interface (green) and second coating interface (dark blue) can be identified. (For interpretation of the references to colour in this figure legend, the reader is referred to the web version of the article.)

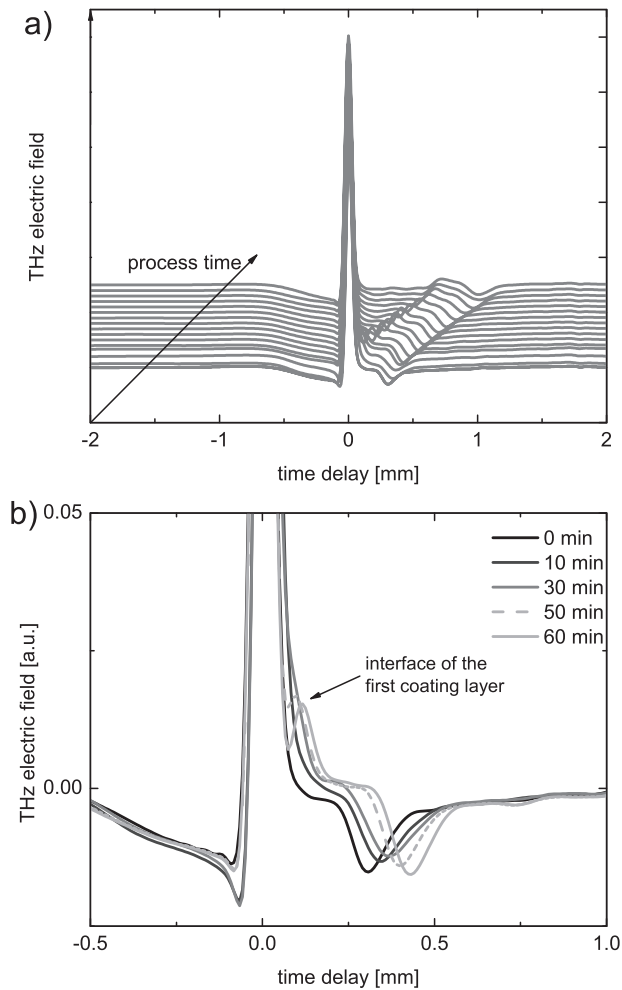


Fig. 4. Average time-domain waveforms acquired by TPI on the yellow tablet face at 0–348 min process time (a). The waveforms are offset in y-direction for clarity. The first coating interface becomes apparent at 50 min process time, i.e. approximately 50 μm coating thickness (b).

A linear correlation with CAN content was found for both the TPI and microscopy measurements. The TPI and microscopy thickness data show a linear correlation among each other despite the deformation of the coating layer during sample preparation in

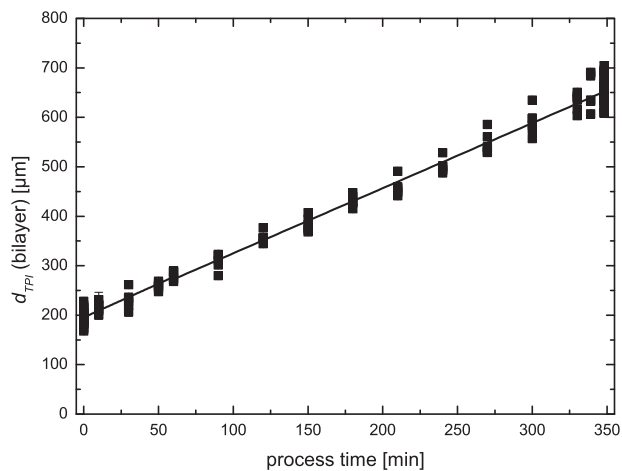


Fig. 5. Increasing joint coating thickness of the two coating layers over process time. Data points show mean \pm s for the individual tablet faces. The linear regression is given in Table 2.

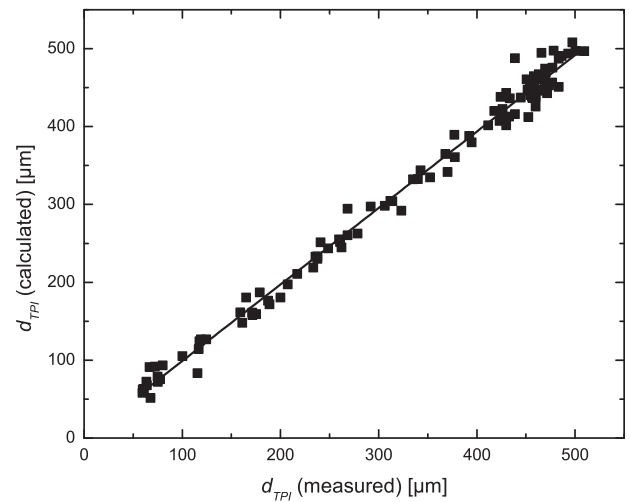


Fig. 6. Comparison of coating thickness values analysing only the active coating layer (x-axis) and analysing both coating layers with subtraction of the y-intercept (y-axis). Data points show mean coating thickness for the individual tablet faces.

microscopy. The highest correlation was found between TPI and CAN content data with a value of $r = 0.997$ (Fig. 10).

4. Discussion

The acquired data shows a linear increase of coating thickness over process time over a broad thickness range up to 500 μm coating thickness. The increase in spray rate was detected by an increasing slope in regression lines after 60 min process time (cf. Fig. 2 and Table 2). By exploiting the additional subcoat that was present in this set of samples for the TPI analysis, it was possible to circumvent the TPI detection limit of approximately 50 μm coating thickness. Both techniques, single- and two-layer analysis, showed good agreement regarding the resultant coating thickness values. Differences in thickness data between the two TPI approaches are due to the fact that the actual thickness of the functional coating on the individual tablets was not determined and hence, variability in coating thickness of the functional film coating was neglected. Only the y-intercept of the regression line was subtracted from the two-layer thickness value. Another drawback of this approach is, that the assumption of a constant thickness of the functional coating throughout the active coating process might not be valid. Subtle changes in the layer thickness of the functional coating layer,

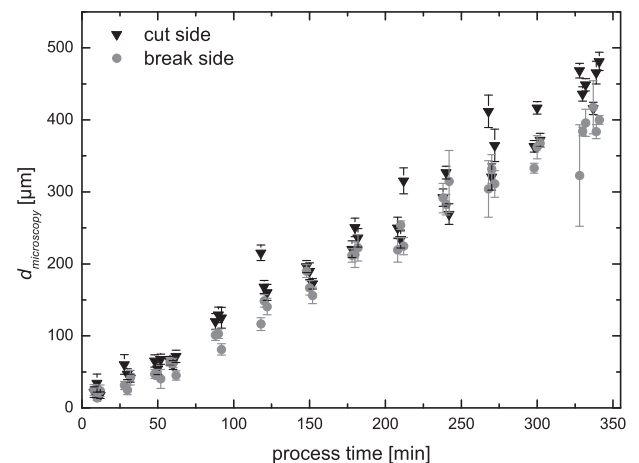


Fig. 7. Coating thickness measured by optical microscopy on cut and break side. Data points show mean \pm s for the individual tablet faces.

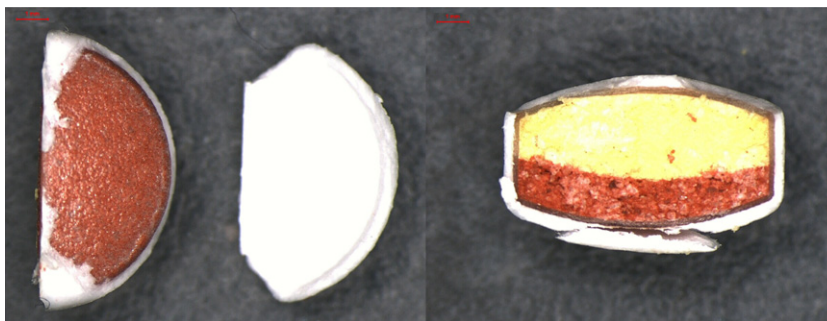


Fig. 8. Sample preparation with liquid nitrogen. Left: complete delamination of active coating layer, right: uneven profile of cross-section.

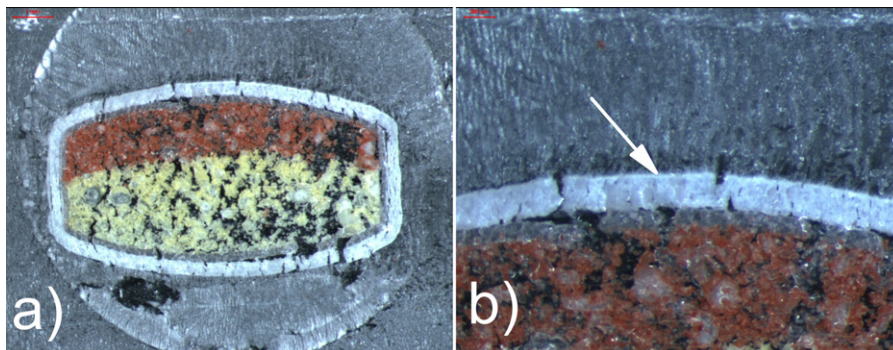


Fig. 9. Cross-section through a tablet prepared with cryomicrotome. Overview (a) and 5-fold magnification (b). Multiple brittle fractures can be found, as well as a beginning dissolution of the active coating layer (red arrow). (For interpretation of the references to colour in this figure legend, the reader is referred to the web version of the article.)

e.g. due to interactions with the active coating or the influence of heat are not taken into account. Furthermore, this approach was only possible for the yellow tablet face. The composition of the red tablet face prevented the detection of the second coating interface as sodium chloride crystals led to strong oscillations in the waveforms at longer delay times, that interfered with the second coating interface. Therefore, the calculation of coating thickness of the functional subcoat was restricted to the yellow tablet face. Another point to consider is, that the real refractive index (n_{real}) of the film coating was unknown and all coating thickness calculations are based on an estimated value of $n_{\text{estimated}} = 1.53$. Therefore, all thickness values are relative and are compared to each other under the assumption, that $n_{\text{estimated}}$ is uniform within the whole batch. Hence, the absolute thickness values are unknown. The correlation of layer thickness values measured by TPI and microscopy

can indicate whether $n_{\text{estimated}}$ approximates to n_{real} . If $n_{\text{estimated}}$ is equal to n_{real} , a slope of 1 is achieved when plotting the thickness data acquired by TPI over the data acquired by microscopy. In the present study a slope of 1.01 was found in the regression analysis (plot not shown). This indicates that n_{real} is only slightly higher than $n_{\text{estimated}}$. However, the deformation of the film coating during the sample preparation for microscopy biases the determination of the layer thickness and consequently, the analysis of the slope can lead to false conclusions regarding the refractive index. Therefore, a suitable technique to accurately determine n still needs to be found, if the real coating thickness values shall be acquired with TPI.

Optical microscopy turned out to be inaccurate in terms of coating thickness measurement, as the film coating deformed during the sample preparation process. An excellent agreement of TPI and microscopy data, as shown by Ho et al. (2007) for a set of much thinner coatings where the effect of plastic deformation might be less significant, could not be confirmed in the present study. Other sample preparation techniques did not improve the quality of the cross sections, leading to the conclusion, that optical microscopy is not an accurate reference method for the investigated dosage form with two coatings of high thickness.

5. Conclusion

In this study, the feasibility of TPI to evaluate the progress of an active coating process was shown in a first proof-of-principle study. Good agreement of the acquired coating thickness data and the CAN content was found over a broad range of coating thickness. Furthermore, it was possible to follow the active coating process from the beginning and to circumvent the detection limit due to the special structure of the dosage form. TPI, as a nondestructive technique, was superior to optical microscopy regarding the determination of coating thickness, as artefacts due to sample preparation could be avoided.

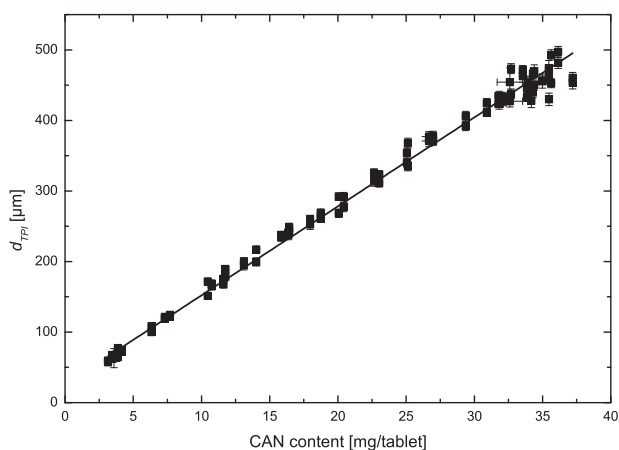


Fig. 10. Correlation of CAN content and coating thickness measured by TPI. Data points show mean \pm s for the individual tablet faces.

Still, some shortcomings were identified. Coating thickness analysis was not possible for all existing layers as the shape of the THz time-domain signals strongly depended on the structure of the tablet core.

The high correlation of CAN content and coating thickness measured by TPI raises the idea to use TPI as a PAT tool to follow the coating process and to estimate the CAN content at different time points during the coating process. Still, the correlation of CAN content and coating thickness in a narrower range needs to be investigated. Provided a good correlation can be achieved, TPI could be used as a tool to predict the actual CAN content throughout the coating process by means of an in-line gauge as demonstrated by May et al. (2011) for a polymer film coating. Furthermore it could give information on content uniformity of the end product. With this it could be used to estimate the outcome of the test on uniformity of dosage units according to the pharmacopoeia.

The TPI layer thickness measurement is directly based on the physical properties of the sample microstructure rather than relying on any chemical information from the coating layer. This makes the TPI approach very versatile as the method can easily be transferred to any other active coating process.

Acknowledgements

The authors would like to thank Wolfram Steinke and Daniela Asmussen from Bayer Pharma AG, Monheim for the preparation of the cryomicrotome cuts and Annemarie Schmitz from the University of Düsseldorf for the HPLC method transfer.

References

- Barcomb, R., 1997. Controlled release of steroids from sugar coatings. EP0803250A1.
- De Beer, T., Burggraeve, A., Fonteyne, M., Saerens, L., Remon, J.P., Vervaeke, C., 2011. Near infrared and Raman spectroscopy for the in-process monitoring of pharmaceutical production processes. *Int. J. Pharm.* 417, 32–47.
- Fricke, S., 2006. Feste perorale Arzneiform zur Kontrazeption, die Dienogest und Ethinylestradiol enthält. EP1690529A1.
- Gendre, C., Genty, M., Boiret, M., Julien, M., Meunier, L., Lecoq, O., Baron, M., Chaminate, P., Péan, J.M., 2011. Development of a process analytical technology (PAT) for in-line monitoring of film thickness and mass of coating materials during a pan coating operation. *Eur. J. Pharm. Sci.* 43, 244–250.
- Ho, L., Müller, R., Gordon, K.C., Kleinebudde, P., Pepper, M., Rades, T., Shen, Y.C., Taday, P.F., Zeitler, J.A., 2009. Monitoring the film coating unit operation and predicting drug dissolution using terahertz pulsed imaging. *J. Pharm. Sci.* 98, 4866–4876.
- Ho, L., Müller, R., Römer, M., Gordon, K.C., Heinämäki, J., Kleinebudde, P., Pepper, M., Rades, T., Shen, Y.C., Strachan, C.J., Taday, P.F., Zeitler, J.A., 2007. Analysis of sustained-release tablet film coats using terahertz pulsed imaging. *J. Control. Release* 119, 253–261.
- May, R.K., Evans, M.J., Zhong, S., Warr, I., Gladden, L.F., Shen, Y., Zeitler, J.A., 2011. Terahertz in-line sensor for direct coating thickness measurement of individual tablets during film coating in real-time. *J. Pharm. Sci.* 100, 1535–1544.
- Müller, J., Knop, K., Thies, J., Uerpmann, C., Kleinebudde, P., 2010a. Feasibility of Raman spectroscopy as PAT tool in active coating. *Drug Dev. Ind. Pharm.* 36, 234–243.
- Müller, J., Knop, K., Wirges, M., Kleinebudde, P., 2010b. Validation of Raman spectroscopic procedures in agreement with ICH guideline Q2 with considering the transfer to real time monitoring of an active coating process. *J. Pharm. Biomed. Anal.* 53, 884–894.
- Zeitler, J.A., Shen, Y., Baker, C., Taday, P.F., Pepper, M., Rades, T., 2007a. Analysis of coating structures and interfaces in solid oral dosage forms by three dimensional terahertz pulsed imaging. *J. Pharm. Sci.* 96, 330–340.
- Zeitler, J.A., Taday, P.F., Newnham, D.A., Pepper, M., Gordon, K.C., Rades, T., 2007b. Terahertz pulsed spectroscopy and imaging in the pharmaceutical setting – a review. *J. Pharm. Pharmacol.* 59, 209–223.